Article

Biodegradable and pH-Responsive Acetalated Dextran (Ac-Dex) Nanoparticles for NIR-Imaging and Controlled Delivery of a Platinum-based Prodrug into Cancer Cells

Carolyne B. Braga, Gabriel Perli, Tiago B. Becher, and Catia Ornelas

Mol. Pharmaceutics, **Just Accepted Manuscript** • DOI: 10.1021/acs.molpharmaceut.9b00058 • Publication Date (Web): 22 Mar 2019

Molecular Pharmaceutics Article

Biodegradable and pH-Responsive Acetalated Dextran (Ac-Dex) Nanoparticles for NIR-Imaging and Controlled Delivery of a Platinum-based Prodrug into Cancer Cells

Carolyne B. Braga, Gabriel Perli, Tiago B. Becher, Catia Ornelas*

Institute of Chemistry, University of Campinas - UNICAMP, 13083-970, Campinas, SP, Brazil

ABSTRACT: Nanoparticles based on the biodegradable acetalated dextran polymer (Ac-Dex) were used for NIR-imaging and controlled delivery of a Pt^{IV} prodrug into cancer cells. The Ac-Dex NPs loaded with the hydrophobic Pt^{IV} prodrug **3** (Pt^{IV}/Ac–Dex NPs) and with the novel hydrophobic NIR-fluorescent dye **9** (NIR-dye9/Ac-Dex NPs), as well as Ac-Dex NPs co-loaded with both compounds (co-loaded Ac-Dex NPs), were assembled using a single oil-in-water nanoemulsion method. Dynamic light scattering (DLS) measurements and scanning electron microscopy (SEM) images showed that the resulting Ac-Dex NPs are spherical with an average diameter of 100 nm, which is suitable for accumulation in tumors via the EPR effect. The new nanosystems exhibited high drug loading capability, high encapsulation efficiency, high stability in physiological conditions, and pH-responsiveness. Drug release studies clearly showed that the Pt^{IV} prodrug **3** release from Ac-Dex NPs was negligible at pH 7.4, whereas at pH 5.5 this compound was completely released with a controlled rate. Confocal laser scanning microscopy (CLSM) unambiguously showed that the NIR-dye 9/Ac-Dex NPs were efficiently uptaken by MCF-7 cells, and cytotoxicity assays against several cell lines showed no significant toxicity of blank Ac-Dex NPs up to 1 mg mL^{-1}. The IC_{50} values obtained for the Pt^{IV} prodrug encapsulated in Ac-Dex NPs was much lower when comparing with the IC_{50} values obtained for the free Pt^{IV} complex and cisplatin, in all cell lines tested. Overall, our results demonstrate, for the first time, that Ac-Dex NPs are a promising drug delivery platform for cancer therapy.

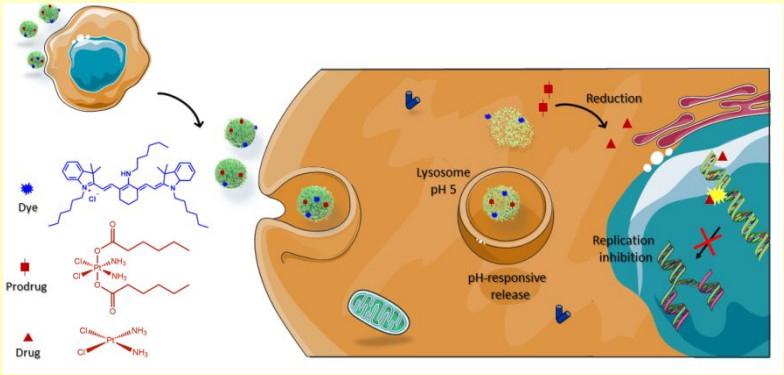

KEYWORDS: *acetalated dextran, polymeric nanoparticles, drug delivery, NIR-imaging, prodrug, nanomedicine*

1. INTRODUCTION

In the last decades, there have been remarkable advances in modern medical sciences, in particular with the development of nanomedicine.[1-3] Despite of the significant improvements in cancer treatments, the number of cancer-related deaths has continued to rise.[4] Current chemotherapy uses nonselective anticancer agents that are not able to differentiate between healthy and cancer cells, causing harmful side effects in patients. These undesirable side effects often limit the doses of chemotherapeutic agents administered to patients, compromising the treatment effectiveness, and contributing to the development of drug resistance, which is also responsible for failure in cancer therapy. Recent research has focused on the development of innovative nanomaterials that aim at selective delivery of chemotherapeutic agents to tumor cells to avoid or decrease the harmful side effects of conventional drugs. The driving force behind this paradigm shift in cancer research is that nanomaterial-based drug delivery systems can dramatically increase the selective drug accumulation in tumor tissues *via* the enhanced permeation and retention effect (EPR effect) or active targeting, thereby reducing the adverse effects while increasing the therapeutic efficacy. Other significant advantages of nanosystems over their free drug counterparts include their ability to increase the drug bioavailability, stability, biodistribution and circulating half-life, resulting in improvements on the drug therapeutic efficacy.[5, 6]

A variety of nanomaterials with potential applications in nanomedicine can be found in the literature, including liposomes,[7, 8] dendrimers,[9-14] hydrogels,[15, 16] polymeric nanoparticles,[17, 18] metallic nanoparticles,[19, 20] quantum dots,[21] mechanized nanoparticles,[22, 23] and polyrotaxanes.[24] Despite the significant progress in the application of nanomaterials in drug delivery applications, numerous opportunities remain for the development of innovative nanotherapeutic systems.

Polymeric nanoparticles are able to carry drugs either by stimuli-responsive covalent attachment or encapsulation within its hydrophobic nanoenvironments or cavity.[17, 25-28] Nanoparticles (NPs) based on biodegradable polymers, such as poly(glycolic acid) (PGA), poly(lactic acid) (PLA), poly(lactic-co-glycolic acid) (PLGA), poly(caprolactone) (PCL), chitosan or hyaluronic acid have been widely explored for the targeted delivery of chemotherapeutics in cancer research. These materials are very attractive especially due to their biodegradability, versatility, biocompatibility, and capability of sustained release, which are crucial properties of drug delivery systems to improve the pharmokinetics of anticancer drugs and to minimize their negative side effects.

Acetalated dextran (Ac-Dex) is a biodegradable polymer that has emerged as a potential candidate for drug delivery applications.[29] In addition to biodegradability, this polymer presents a variety of interesting features, including facile synthesis, pH-responsiveness, controlled release, high loadings, high biocompatibility and versatility, and functionalization capability.[30] Ac-Dex is prepared through a one-step synthesis from the clinically approved biopolymer dextran, a homopolysaccharide of glucose. Protection of the pendant hydroxyl groups of water-soluble dextran with acetal groups affords the hydrophobic Ac-Dex polymer containing both cyclic and acyclic acetal groups (Scheme 1).[29, 31] This acetalated polymer exhibits a pH-responsive degradation, since acetal groups undergo hydrolysis under mildly acidic conditions (pH 5.5), converting back to its hydrophilic and biocompatible precursor dextran.[29, 32]

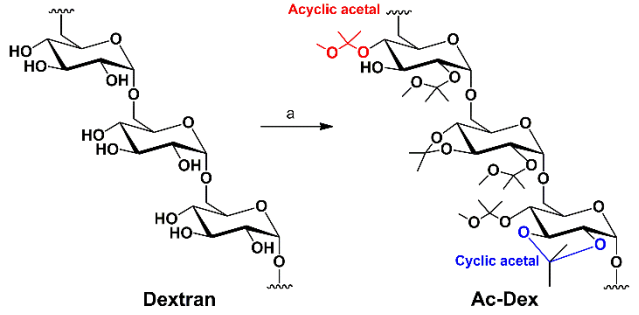

Scheme 1. Synthesis of hydrophobic acetalated dextran (Ac-Dex) polymer from natural polyssacharide dextran: (a) 2-methoxypropene, pyridinium *p*-toluenesulfonate, DMSO.[29]

Ac-Dex polymer has been tailored into micro- and nanoparticles by using standard emulsion methods. Depending on the emulsion approach employed, oil-in-water (o/w) or water-in-oil-in-water (w/o/w), the resulting particles have been used to encapsulate hydrophobic or hydrophilic compounds, respectively.

The uniqueness of this modified-dextran polymer over other pH-sensitive polymers comes from its highly tunable degradation rate, which is dependent on the ratio between the two different types of acid-labile acetal groups (cyclic and acyclic) on its structure. The ratio of cyclic and acyclic acetals is tailored by the acetalation reaction kinetics, since longer reaction times produce the thermodynamically more stable cyclic acetals.[31] Thus, Ac-Dex particles are very attractive for drug delivery applications because the release rate of the encapsulated therapeutic agent from Ac-Dex particles can be tailored according to the desired application.

Several studies have explored the pH-responsive Ac-Dex micro- or nanoparticles as a delivery vehicle for therapeutic agents including proteins,[29, 31, 33] peptides,[34, 35] small molecules,[36, 37] antibiotics,[38] and nucleotides.[39, 40] For example, Ac-Dex NPs were able to encapsulate hydrophobic silver carbenes in relatively high loadings, and showed significant antimicrobial activity against both gram-positive and gram-negative bacteria.[38] More recently, Bachelder *et al.* have shown that Ac-Dex microparticles facilitated delivery of the host-directed therapeutic AR-12 to clear intracellular infections within phagocytes.[41] However, there are no studies on the use of Ac-Dex nanoparticles as drug delivery systems for anticancer drugs. The lability of the acetal groups on Ac-Dex at pH 5.5 make it an attractive candidate for the selective delivery of anticancer agents to tumor cells.

Here we describe, for the first time, the use of Ac-Dex NPs for both imaging and delivery of an anticancer prodrug to cancer cells. The Ac-Dex NPs were tailored with an average size of 100 nm in order to enhance the drug pharmokinetics and to enable accumulation in tumor cells *via* the EPR effect. The hydrophobic Pt^{IV} prodrug *cis,cis,trans*-$[Pt(NH_3)_2Cl_2(CO_2(CH_2)_4CH_3)_2]$ was chosen as the anticancer agent due to its low cytotoxicity and known ability to be reduced intracellularly into highly cytotoxic Pt^{II} species (cisplatin).[42-44] This strategy of using an inert cisplatin prodrug improves cisplatin tolerability and efficacy *in vivo*. The single nanoemulsion method used to encapsulate hydrophobic molecules in Ac-Dex nanoparticles was further explored to encapsulate the new hydrophobic NIR-dye to provide nanoparticles suitable for NIR-imaging, and to co-encapsulate the Pt^{IV} prodrug and the NIR-dye to provide nanoparticles with the dual role of imaging and treating, providing a system suitable for theranostic applications.[45, 46]

2. EXPERIMENTAL SECTION

2.1. General Considerations. Cell counting kit 8 (CCK-8), dextran (from *Leuconostoc mesenteroides*; average MW 9000-1100) and all chemical reagents were purchased from Sigma-Aldrich and used without further purification unless otherwise noted. DMSO was purchased anhydrous (> 99.9%) and used under nitrogen atmosphere; all other solvents were analytical grade and were used as supplied. DMEM, RPMI-1640 and 0.25% trypsin-EDTA solution were purchased from Gibco®. Fetal bovine serum (FBS) and Dulbecco modified phosphate buffered saline (DMPBS, pH 7.4) were purchased from Nutricell Nutrientes Celulares (Campinas, SP, Brazil). Hoechst 33342 and Alexa Fluor® 555 Phalloidin were obtained from Life Technologies. dd-H_2O (pH 8.0) was prepared

using NaOH and/or HCl to adjust pH, and pH was always checked prior to each use.

2.2. Synthesis of Acetalated Dextran Polymer (Ac-Dex). The Ac-Dex polymer was synthesized in one step from dextran following a previously published procedure.[29] The detailed procedure is described in the Supporting Information.[31]

2.3. Synthesis of Pt^{IV} complex and its percursors. Cisplatin was purchased from Sigma-Aldrich, and was oxidized using hydrogen peroxide to afford the compound **2**.[47, 48] The resulting Pt^{IV} complex **2** reacted with hexanoic anhydride to yield the hydrophobic Pt^{IV} prodrug **3**.[49] The detailed synthetic procedures are described in the Supporting Information.

2.4. Synthesis of NIR-dye 9 and its precursors.

2.4.1. Synthesis of N-[5-anilino-3-chloro-2,4-(propane-1,3-diyil)-2,4-pentadiene-1-ylidene]anilinium chloride (5). Phosphorus oxychloride ($POCl_3$, 1.1 mL, 11.80 mmol) was added dropwise to anhydrous DMF (1.3 mL, 16.79 mmol) in an ice bath at 0 ºC. After 30 min, cyclohexanone (**4**) (0.6 mL, 5.79 mmol) was added dropwise, and the reaction mixture was refluxed for 1 h under nitrogen atmosphere. The reaction mixture was cooled to room temperature. A solution of aniline (0.9 mL) in ethanol (100 mL) was added dropwise, and the reaction mixture was stirred for further 1 h. The resulting deep purple mixture was poured into 1 L of ice cold HCl aqueous solution (10%), and the product was allowed to crystallize overnight at 4 ºC. The crystals were filtered off, washed twice with ice-cold water, and once with diethyl ether, and then dried under vacuum. Compound **5** was obtained as purple crystals in 63% yield (1.3 g, 3.62 mmol). ^{1}H NMR (400 MHz, DMSO–d_6), δ (ppm): 8.54 (s, 2H, $^+$NC*H*), 7.56 (m, 4H, arom. H), 7.47 (m, 4H, arom. H), 7.28 (m, 2H, arom. H), 2.73 (t, J = 6.0 Hz, 4H, $^+$NCCCH_2), 1.87 (quint, J = 6.0 Hz, 2H, $^+$NCCCCH_2). HRMS (ESI+) m/z $[M]^+$ calcd for $C_{20}H_{20}ClN_2^+$: 323.1309, found: 323.1252.

2.4.2. Synthesis of 1-hexyl-2,3,3-trimethyl-3H-indol-1-ium iodide (7).[50] A mixture of 1-iodohexane (3.2 g, 15.09 mmol) and 2,3,3-trimethylindolinine (2.0 g, 12.56 mmol) in acetonitrile was refluxed with continuous stirring for 16 h to produce a pink solution. The reaction mixture was cooled to room temperature and the solvent was evaporated. The crude product was dissolved in a minimum amount of dichloromethane (1.5 mL) and poured over 400 mL of diethyl ether under vigorous stirring. The precipitate obtained was washed with diethyl ether (20 mL x 3) and dried under vacuum to give 4.1 g of pure compound **7** (11.04 mmol, 88%) as a purple solid. ^{1}H NMR (400 MHz, DMSO–d_6), δ (ppm): 7.98 (m, 1H, arom. H), 7.84 (m, 1H, arom. H), 7.62 (m, 2H, arom. H), 4.46 (t, J = 7.8 Hz, 2H, $^+$NCH_2(CH$_2$)$_4$CH$_3$), 2.86 (s, 3H, $^+$NCCH_3), 1.83 (quint, J = 7.8 Hz, 2H, $^+$NCH$_2$CH_2(CH$_2$)$_3$CH$_3$), 1.54 (s, 6H, $^+$NCC(CH_3)$_2$), 1.41 (m, 2H, $^+$N(CH$_2$)$_2$CH_2(CH$_2$)$_2$CH$_3$), 1.28 (m, 4H, $^+$N(CH$_2$)$_3$(CH_2)$_2$CH$_3$), 0.85 (t, J = 7.0 Hz, 3H, $^+$N(CH$_2$)$_5$CH_3). ^{13}C NMR (100 MHz, DMSO–d_6), δ (ppm): 196.9 ($^+$N*C*CH$_3$), 142.3 (arom. $^+$N*C*$_q$), 141.5 (arom. $^+$NC$_q$*C*$_q$), 129.9 (arom. *C*H), 129.5 (arom. *C*H), 124.0 (arom. *C*H), 116.0 (arom. *C*H), 54.7 ($^+$N*C*H$_2$(CH$_2$)$_4$CH$_3$), 48.2 ($^+$NC*C*(CH$_3$)$_2$), 31.2 ($^+$NCH$_2$*C*H$_2$(CH$_2$)$_3$CH$_3$), 27.7 ($^+$N(CH$_2$)$_2$*C*H$_2$(CH$_2$)$_2$CH$_3$), 26.0 ($^+$N(CH$_2$)$_3$*C*H$_2$CH$_2$CH$_3$), 22.5 ($^+$NCC(*C*H$_3$)$_2$), 22.3 ($^+$N(CH$_2$)$_4$*C*H$_2$CH$_3$), 14.7 ($^+$N(CH$_2$)$_5$*C*H$_3$), 14.3 ($^+$NC*C*H$_3$). HRMS (ESI+) m/z $[M^+]$ calcd for $C_{17}H_{26}N^+$: 244.2060, found: 244.1987.

2.4.3. Synthesis of chlorocyanine dye 8. To a solution of iminium salt **5** (0.6 g, 1.71 mmol) and indolium derivative **7** (1.3 g, 3.40 mmol) in absolute ethanol (50 mL), anhydrous sodium acetate (320 mg, 3.97 mmol) was added. The resulting mixture was refluxed for 12 h under nitrogen atmosphere. The ethanol was removed under reduced pressure after completion of reaction. The crude product was purified by column chromatography over silica gel with acetone/methanol (95:5) as eluent to afford 1.1 g of **8** (1.67 mmol, 98%) as a deep green solid. ^{1}H NMR (400 MHz, DMSO-d_6), δ (ppm): 8.26 (d, J = 14.0 Hz, 2H, $^+$NCC*H*), 7.64 (d, 2H, arom. H), 7.45 (m, 4H, arom. H), 7.29 (m, 2H, arom. H), 6.34 (d, J = 14.2 Hz, 2H, $^+$NCCHC*H*), 4.23 (m, 4H, $^+$NCH_2(CH$_2$)$_4$CH$_3$), 2.72 (m, 4H, ClCCCH_2), 1.88 (m, 2H, ClCCCH$_2$CH_2), 1.75 (m, 4H, $^+$NCH$_2$CH_2(CH$_2$)$_3$CH$_3$), 1.68 (s, 12 H, $^+$NCC(CH_3)$_2$), 1.41-1.27 (m, 12H, $^+$N(CH$_2$)$_2$CH_2CH_2CH_2CH$_3$), 0.86 (t, 6H, $^+$N(CH$_2$)$_5$CH_3). ^{13}C NMR (100 MHz, DMSO-d_6), δ (ppm): 172.7 ($^+$N*C*C(CH$_3$)$_2$), 143.4 (arom. $^+$N*C*$_q$), 142.5 (arom. $^+$NC$_q$*C*$_q$), 141.5 ($^+$NCCHCH*C*CCl), 132.0 ($^+$NCCH*C*HCCCl), 129.1 (arom. *C*H), 126.6 (Cl*C*), 125.7 (arom. *C*H), 123.0 (arom. *C*H), 112.0 (arom. *C*H), 102.1 ($^+$NC*C*HCHCCCl), 49.5 ($^+$NC*C*(CH$_3$)$_2$), 44.3 ($^+$N*C*H$_2$(CH$_2$)$_4$CH$_3$), 31.3 ($^+$NCH$_2$*C*H$_2$(CH$_2$)$_3$CH$_3$), 27.9 (ClCC*C*H$_2$CH$_2$), 27.7 (ClCCCH$_2$*C*H$_2$), 27.4 ($^+$N(CH$_2$)$_2$*C*H$_2$(CH$_2$)$_2$CH$_3$), 26.2 ($^+$N(CH$_2$)$_3$*C*H$_2$CH$_2$CH$_3$), 22.4 ($^+$NCC(*C*H$_3$)$_2$), 19.3 ($^+$N(CH$_2$)$_4$*C*H$_2$CH$_3$), 14.3 ($^+$N(CH$_2$)$_5$*C*H$_3$). HRMS (ESI+) m/z $[M]^+$ calcd for $C_{42}H_{56}ClN_2^+$: 623.4127, found: 623.4069.

2.4.4. Synthesis of aminocyanine dye 9. Dye **8** (1.5 g, 2.27 mmol) and hexylamine (394.6 mg, 3.90 mmol) were dissolved in anhydrous DMF (25 mL), and the solution was heated at 80 ºC for, 16 h. The solution color gradually changed from green to deep blue. The solvent was removed under vacuum and the product was purified by column chromatography using silica gel and acetone/methanol (99:1) as eluent. Dye **9** was obtained as a deep blue solid in 67% yield (1.1 g, 1.52 mmol). ^{1}H NMR (400 MHz, DMSO–d_6), δ (ppm): 7.72 (d, J = 12.7 Hz, 2H, $^+$NCC*H*), 7.27 (m, 4H, arom. H), 7.05 (m, 2H, arom. H), 6.83 (m, 2H, arom. H), 5.59 (d, J = 12.7 Hz, 2H, $^+$NCCHC*H*), 3.88 (m, 2H, NHCH_2(CH$_2$)$_4$CH$_3$), 3.78 (m, 4H, $^+$NCH_2(CH$_2$)$_4$CH$_3$), 2.47 (t, 4H, NHCCCH_2), 1.97 (quint, 2H, NHCH$_2$CH_2(CH$_2$)$_3$CH$_3$), 1.82 (m, 2H, NHCCCH$_2$CH_2), 1.75 (m, 4H, $^+$NCH$_2$CH_2(CH$_2$)$_3$CH$_3$), 1.70 (s, 12 H, $^+$NCC(CH_3)$_2$), 1.47-1.26 (m, 18H, $^+$N(CH$_2$)$_2$(CH_2)$_3$CH$_3$ and NH(CH$_2$)$_2$(CH_2)$_3$CH$_3$), 0.91 (t, 6H, $^+$N(CH$_2$)$_5$CH_3), 0.87 (t, 3H, NH(CH$_2$)$_5$CH_3). ^{13}C NMR (100 MHz, DMSO–d_6), δ (ppm): 169.2 ($^+$N*C*C(CH$_3$)$_2$), 166.9 ($^+$NCCHCHC*C*NH),

143.2 (arom. $^{+}NC_q$), 140.1 (arom. $^{+}NC_qC_q$), 138.0 ($^{+}$NCCHCH*C*CNH), 128.0 ($^{+}$NCCH*C*HCCNH), 122.5 (arom. *C*H), 122.0 (arom. *C*H), 120.1 (arom. *C*H), 108.22 (arom. *C*H), 94.0 ($^{+}$NC*C*HCHCCNH), 50.1 ($^{+}N\mathit{C}H_2(CH_2)_4CH_3$), 47.7 ($^{+}NC\mathit{C}(CH_3)_2$), 43.2 ($NH\mathit{C}H_2(CH_2)_4CH_3$), 31.5 and 31.4 ($^{+}NCH_2\mathit{C}H_2(CH_2)_3CH_3$ and $NHCH_2\mathit{C}H_2(CH_2)_3CH_3$), 29.1 ($^{+}NCC(\mathit{C}H_3)_2$ and $NHCCC\mathit{H}_2CH_2$), 26.8, 26.5 and 26.4 ($NHCCCH_2\mathit{C}H_2$, $^{+}N(CH_2)_2\mathit{C}H_2(CH_2)_2CH_3$ and $NH(CH_2)_2\mathit{C}H_2(CH_2)_2CH_3$), 25.2 ($^{+}N(CH_2)_3\mathit{C}H_2CH_2CH_3$), 22.6, 22.5 and 21.6 ($^{+}N(CH_2)_4CH_2CH_3$, $NH(CH_2)_3\mathit{C}H_2CH_2CH_3$ and $NH(CH_2)_4CH_2CH_3$), 14.1 and 14.0 ($^{+}N(CH_2)_5\mathit{C}H_3$ and $NH(CH_2)_5\mathit{C}H_3$). HRMS (ESI+) *m/z* $[M]^+$ calcd for $C_{48}H_{70}N_3^+$: 688.5564, found: 688.5483.

2.5. Preparation of empty Ac-Dex NPs (Blank Ac-Dex NPs). The preparation of blank Ac-Dex NPs was performed by adapting the oil-in-water (o/w) nanoemulsion solvent evaporation procedure described by Ornelas *et al*.[38] Ac-Dex (25 mg) dissolved in 1 mL of ethyl acetate was added to 5 mL of polyvinyl alcohol (PVA; MW 13,000-23,000 g/mol, 87–89% hydrolyzed) solution (3% wt/wt in PBS). The mixture was emulsified through ultrasonication for 30 s in an ice bath by using a probe sonicator (Branson Digital Sonifier 250) with 0.5 s pulses intercalated with 0.1 s intervals, and amplitude of 50%. A white milky solution was obtained, and the organic solvent was evaporated under a gentle flow of dry nitrogen for 2 h. Nanoparticles were isolated by centrifugation (6,500 × g, 30 min), and washed with dd-H_2O (pH 8.0). Three cycles of redispersion in dd–H_2O (5 mL, pH 8.0), vortexing, bath sonication (15-20 min), centrifugation (6,500 × g, 20 min) and removal of supernatant were performed. Finally, residual water was removed under vacuum to yield a white fluffy powder (13 mg).

2.6. Preparation of Ac-Dex NPs encapsulating the Pt^{IV} Prodrug 3 (Pt^{IV}/Ac-Dex NPs). Pt^{IV}-loaded Ac-Dex NPs were prepared following a similar procedure to that described for blank NPs. In this case, 7.5 mg of the Pt^{IV} compound **3** (corresponding to an initial feed of 30% (w/w), defined as (mg of Pt^{IV} complex/mg of polymer) × 100) was dissolved in the organic phase together with Ac-Dex prior to sonication.

2.7. Preparation of Ac-Dex NPs encapsulating the NIR dye 9 (NIR dye 9/Ac-Dex NPs). Dye **9**-loaded Ac-Dex NPs were prepared in the same manner as Pt^{IV}/Ac-Dex NPs, but in this case dichloromethane was used as the organic solvent instead of ethyl acetate.

2.8. Preparation of Ac-Dex NPs co-encapsulating the Pt^{IV} Prodrug 3 and the NIR-dye 9 (co-loaded Ac-Dex NPs). Co-loaded Ac-Dex NPs were prepared in a similar manner as the single loaded Ac-Dex NPs, but in this case both 7.5 mg of Pt^{IV} compound **3** and 0.5 mg of dye **9** were dissolved in ethyl acetate together Ac-Dex prior to sonication.

2.9. Nanoparticle Size, Polydispersity Index and Zeta Potential. Particle's hydrodynamic diameter, polydispersity index (PDI) and zeta potential were determined by dynamic light scattering (DLS). Measurements were carried out at 25 ºC on a Zetasizer Nano-ZS ZEN3600 instrument (Malvern Instruments) equipped with a 4 mW He–Ne laser with light wavelength of 632.8 nm, and backscattering angle of 173°, using a disposable DTS 1070 cell. Nanoparticle samples were dispersed in dd-H_2O (pH 8.0) at a concentration of 1 $mg.mL^{-1}$ and each sample was analyzed in triplicate. Data are presented as % by number.

2.10. Surface Morphology. The surface morphology of Ac-Dex NPs was examined using a Quanta 250 field emission scanning electron microscope (FESEM) (FEI Ltd.) operating at an accelerating voltage of 5 kV. Particle samples were prepared by dropping 10 µL of a nanoparticle suspension (1 $mg.mL^{-1}$ in dd-H_2O, pH 8.0) onto a polished silicon wafer. Samples were allowed to dry overnight in the air, and sputter coated with a layer of iridium in a Bal-Tec MD 020 instrument (Balzers).

2.11. Quantification of Pt^{IV} complex 3 encapsulated in Ac-Dex NPs. The concentration of compound **3** encapsulated in the Ac-Dex NPs (Pt^{IV}/Ac-Dex NPs and co-loaded/Ac-Dex NPs) was determined by inductively coupled plasma-optical emission spectroscopy (ICP-OES) measurements of free platinum using a Perkin Elmer Optima 8300 optical emission spectrometer. Samples were prepared through digesting the nanoparticle suspensions in HNO_3 and diluting in Milli-Q water to a final acid content of 2%. Intensity of spectral line at 265.945 nm was measured for all samples and standards. The platinum concentration in the samples was determined by comparing the measured intensity with a calibration curve of platinum. All ICP-OES measurements were carried out in triplicate.

2.12. Quantification of dye 9 encapsulated in Ac-Dex NPs. The amount of dye **9** encapsulated in the NIR-dye **9**/Ac-Dex NPs and co-loaded/Ac-Dex NPs was determined using an UV-vis spectrometer (Agilent HP 8453). The particles were weighted out in triplicate and dissolved in THF to release the cargo. Then, the absorbance of dye **9** at 633 nm was measured, and its concentration in solution was calculated from a pre-established calibration curve. All UV-vis measurements were carried out in triplicate.

2.13. Loading Content and Encapsulation Efficiency. The loading content (LC) and encapsulation efficiency (EE) of the nanoparticles were calculated as follows:

$$\text{LC \%} = \frac{weight\ of\ compound\ encapsulated\ in\ nanoparticles}{total\ weight\ of\ nanoparticles} \times 100$$

$$\text{EE \%} = \frac{weight\ of\ compound\ encapsulated\ in\ nanoparticles}{total\ weight\ of\ compound} \times 100$$

2.14. Stability Study. The physical stability of Ac-Dex NPs was evaluated by monitoring the changes in their size over time. Particles were incubated under mildly basic (dd-H_2O, pH 8.0) and acidic (0.1 M acetate buffer pH 5.5), and physiological conditions (0.01 M PBS buffer pH 7.4 and DMEM containing 10% FBS pH 7.4), at 37 °C with

constant agitation. At determined time points (0, 0.4, 1, 2, 4, 8, 12, 24, 48 and 72 h), the particles' size was monitored by DLS.

2.15. *In Vitro* Release Study. Pt^{IV}/Ac-Dex NPs and NIR-dye **9**/Ac-Dex NPs were suspended in either 3% Tween 80 in 0.1 M acetate buffer (pH 5.5) or 3% Tween 80 in 0.01 M PBS buffer (pH 7.4), and incubated at 37 °C under gentle shaking. At selected time intervals (0, 2, 4, 6, 8, 12, 24, 48 and 72 h), the suspension was centrifuged at 11,300 × g for 20 min to separate pellet from supernatant. The supernatant was removed and replaced with the same volume of fresh buffer solution containing 3% Tween 80, in which the pellet was resuspended and returned for further incubation. The amount of Pt^{IV} complex **3** and NIR-dye **9** was quantified by ICP-OES and UV-vis spectroscopy, respectively. The cumulative amount of released compound was calculated, and the percentages of compound released from Ac-Dex NPs were plotted against time. The release experiments were conducted in triplicate.

2.16. Cell Culture. The human MCF-7 (breast cancer), PC3 (prostate cancer) and PNT2 (normal prostate) cells were cultured in RPMI-1640 supplemented with 10% FBS and 1% penicillin–streptomycin. HeLa (human cervical cancer) cells were cultured in DMEM (Dulbecco's Modified Eagle Medium) with high glucose supplemented with 10% FBS and 1% penicillin–streptomycin. Caco-2 (human colorectal cancer) cells were maintained in DMEM with high glucose containing 1% nonessential amino acids, 2 mM L–glutamine, 10% FBS and 1% penicillin–streptomycin. All cells were incubated at 37 °C in a humidified atmosphere with 5% CO_2. The cell culture medium was changed every 2-3 days, and cells were passaged at 80-90% confluency using 0.25% trypsin-0.02% EDTA solution.

2.17. *In Vitro* Cellular Uptake Study. Confocal laser scanning microscopy (CLSM) was used to visualize cellular uptake of the NPs. MCF-7 cells were seeded into 6-well plates at a density of 3×10^5 cells/well in 3 mL of RPMI–1640 supplemented with 10% FBS and 1% penicillin–streptomycin. After culturing for 24 h at 37 °C in a humidified atmosphere with 5% CO_2, the cells were further incubated for 6 h with free NIR-dye **9** and with NIR-dye9/Ac-Dex NPs at 0.1 μM (final concentration of dye). The cells were washed three times with PBS, fixed with 4% *p*–formaldehyde for 15 min at room temperature, and washed again with PBS. Then, the cells were permeabilized with 0.2% Triton X-100 for 5 min, washed with PBS, and incubated with Hoechst 33342 to label the nuclei and with Alexa Fluor 555 Phalloidin for staining the cytoskeleton, according to the standard protocol provided by the supplier. The slides containing the cells were rinsed once with PBS and mounted with antifading solution. Finally, the fluorescence images were obtained using an Upright LSM780–NLO Zeiss confocal laser scanning microscope equipped with 405, 458, 488, 514, 543, 561, and 633 nm laser excitation sources. Hoechst 33342 and Alexa Fluor 555 Phalloidin were excited at 405 nm and 543 nm, whereas 633 nm was used to excite dye **9**.

2.18. Cell Viability Assay. Cells were seeded into 96–well plates (7.5×10^3 cells/well) containing 200 μL of complete cell culture medium, and incubated for 24 h at 37 °C in a humidified atmosphere with 5% CO_2. Then, the cells were treated with different concentrations of Pt^{IV}/Ac-Dex NPs (concentration of Pt^{IV} compound **3**: 2.9×10^{-4} - 28.8 μM), NIR-dye**9**/Ac-Dex NPs (concentration of dye **9**: 2.0×10^{-5}- 2.0 μM), and co-loaded Ac-Dex NPs (concentration of Pt^{IV} compound **3**: 2.9×10^{-4} - 28.8 μM and concentration of dye **9**: 2.0×10^{-5}- 2 μM) for further 48 h. Cisplatin, free Pt^{IV} complex and empty Ac-Dex NPs were also tested for comparison, using the same procedure. After incubation, the growth medium was removed, the cells were washed twice with PBS, and the cell viability was evaluated using the Cell Counting Kit-8 (CCK-8) according to the manufacturer's instructions. The absorbance of the solution in each well was measured at 450 nm in a microplate reader (FlashScan 530 Analitic Jena). The negative control was designed as 100% of dehydrogenase activity, and cell viability was expressed as a percentage of the untreated cells.

3. RESULTS AND DISCUSSION

The use of Pt^{IV} prodrugs instead of injecting directly highly toxic Pt^{II} cisplatin has been recently investigated as a potential strategy to overcome resistance of cisplatin and minimize its harmful side effects while maintain its potency against cancer cells. This strategy relies on the fact that Pt^{IV} complexes present low toxicity; however, inside the cells they are reduced by the intracellular medium to highly toxic Pt^{II}.[49] In order to increase the efficiency of anticancer therapy and increase its selectivity while minimizing its harmful side effects, in this study we designed a drug delivery system that combines the advantages of Ac-Dex NPs with the advantages of using a Pt^{IV} prodrug. The current design is expected to provide a nanomaterial system that will be more selective and more effective against cancer cells through EPR effect while being harmless to healthy tissues (Scheme 2).

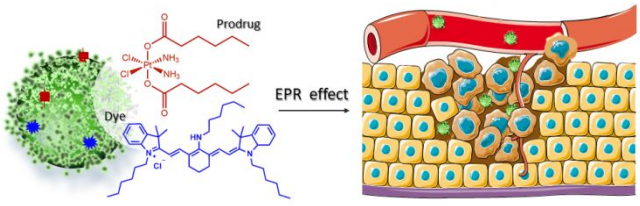

Scheme 2. Schematic representation of the new Ac-Dex drug delivery system for the sustained release of the Pt^{IV} prodrug **3** to cancer cells, and NIR imaging with dye **9**.

3.1. Synthesis and characterization of the hydrophobic Pt^{IV} prodrug 3

Complex *cis*,*cis*,*trans*-$[Pt(NH_3)_2Cl_2(CO_2(CH_2)_4CH_3)_2]$ **3** (Scheme 3) was chosen as the Pt^{IV} prodrug because its hydrophobicity allows encapsulation in Ac-Dex NPs using o/w emulsion procedures, and because this complex is reduced to highly cytotoxic cisplatin by the intracellular medium.[49]

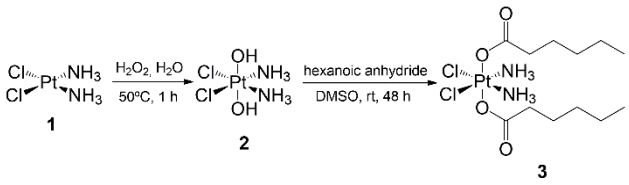

Scheme 3. Synthesis of the hydrophobic Pt^{IV} prodrug **3** using cisplatin (**1**) as starting material. Pt^{II} was oxidized to Pt^{IV} in the presence of hydrogen peroxide, and the resulting compound **2** reacted with hexanoic anhydride to yield the hydrophobic Pt^{IV} complex **3**.

The hydrophobic Pt^{IV} prodrug **3** having two aliphatic carboxylate axial ligands was synthesized from cisplatin **1** in two steps (Scheme 3), with a global yield of 40%. IR and NMR spectroscopies were employed to confirm the structures of **2** and **3**, and the corresponding spectra are shown in Figures S1 to S3 of the Supporting Information (S.I.). Since the compound **3** dissolves in the organic solvent ethyl acetate, it was a suitable candidate for encapsulation in Ac-Dex NPs by single emulsion process.

3.2. Synthesis and characterization of the hydrophobic NIR-fluorescent dye 9

A new hydrophobic dye from the tricarbocyanine family that is fluorescent in the near infrared region (NIR) was synthesized to be efficiently encapsulated in the Ac-Dex NPs by single nanoemulsion process. We focused on the synthesis of a tricarbocyanine dye since this class of compounds have been widely explored as imaging agents due to their strong fluorescence in the NIR region and low cytotoxicity.[51] The synthetic route to synthesize dye **9** involved four steps (Scheme 4).[50, 52]

The precursor *N*-[5-anilino-3-chloro-2,4-(propane-1,3-diyil)-2,4-pentadiene-1-ylidene]anilinium chloride (**5**) was synthesized by Vilsmeier–Haack formylation of cyclohexanone **4**. In parallel, 1-hexyl-2,3,3-trimethyl-3*H*-indol-1-ium iodide (**7**) was prepared by alkylation of 2,3,3-trimethylindolinine (**6**) with hexyl iodide in refluxing acetonitrile. The iminium salt **5** was condensed with the indolium derivative **7** to afford the chlorocyanine dye **8** in 98% yield as a bright green solid**.** Finally, the aminocyanine dye **9** was obtained as a deep blue solid from the $S_{RN}1$ reaction of **8** with hexylamine. All compounds were fully characterized using NMR spectroscopy and high-resolution mass spectrometry (HRMS). The detailed structural characterization of the compounds is provided in Figures S4 to S14 (SI).

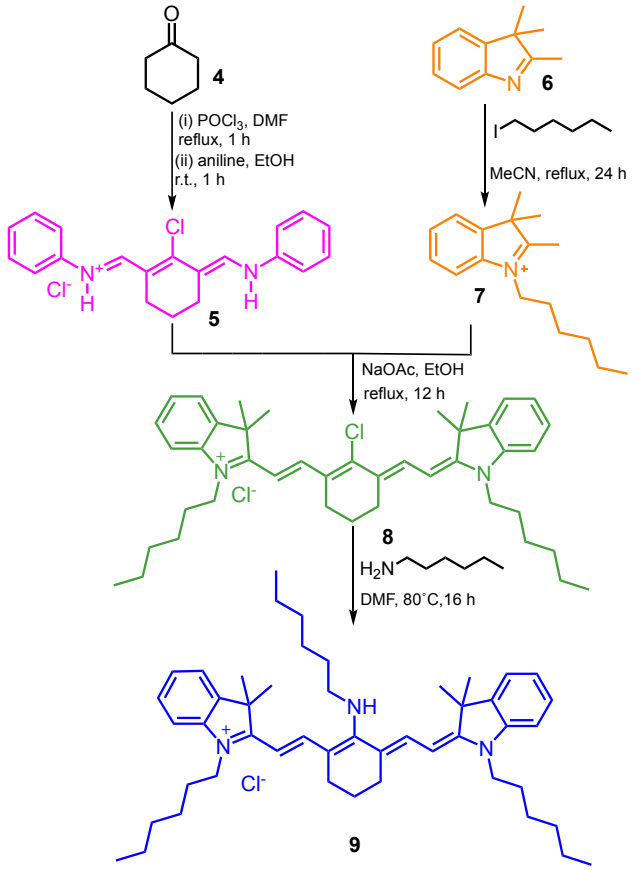

Scheme 4. Synthesis of the hydrophobic NIR-fluorescent aminocyanine dye **9**.

The photophysical properties of dye **9** were evaluated in six different solvents: tetrahydrofuran (THF), chloroform ($CHCl_3$), dichloromethane (DCM), acetonitrile (ACN), dimethylsulfoxide (DMSO) and methanol (MeOH). The UV-vis absorption and emission spectra of the dye **9** are shown in Figure 1, and the relevant data are summarized in Table 1. The absorption spectra of dye **9** in solution showed an absorption band with λ_{max} at around 635 nm. Dye **9** presents a large Stokes shift (ranging from 97 in dichloromethane to 133 in DMSO), which can be attributed to an intramolecular charge transfer (ICT) transition.[52, 53]

Table 1. Photophysical data from absorption and emission[a] spectra of the aminocyanine dye **9** in six solvents.

Solvent	λ_{max} (absorption) (nm)	ε (M^{-1} cm^{-1})	λ_{max} (emission) (nm)	Stokes shift (nm)
THF	633	29503	758	125
$CHCl_3$	635	20329	764	129
DCM	665	79693	762	97
ACN	635	22505	750	115
DMSO	633	81741	766	133
MeOH	633	99394	757	124

[a]Excitation wavelength: 635 nm.

One of the major disadvantages of tricarbocyanine dyes is their tendency to aggregate in solution; however, it is interesting to note that dye **9** has low tendency to aggregate in the tested solvents. The absorption spectra of dye **9** in DCM, ACN, MeOH and DMSO show mainly the absorption band at 635 nm that corresponds to the monomeric species. Only in THF and $CHCl_3$ the absorption spectra show the presence of significant bands at lower wavelengths (hypsochromic shift) that correspond to parallel aggregates, which are known as H-type aggregates.[52] The high molar absorption coefficients (ε) of dye **9** (around $8x10^4$ - $1x10^5$ M^{-1} cm^{-1}) decrease significantly in THF and $CHCl_3$ probably due to the presence of the H-type aggregates. These photophysical properties of dye **9** together with its strong fluorescence in the NIR region are promising features for the use of this dye as an imaging agent when encapsulated in Ac-Dex NPs.

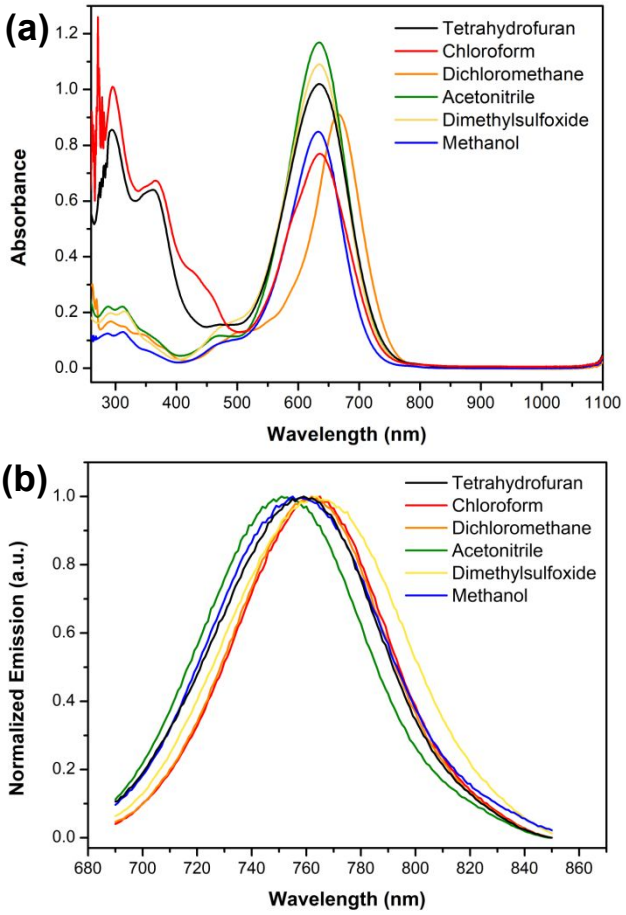

Figure 1. Absorption (a) and emission (b) spectra of dye **9** in six different solvents.

3.3. Preparation and characterization of Ac-Dex NPs

Ac-Dex NPs were tailored to enhance tumor accumulation and to release the encapsulated prodrug in a sustained manner within 12 h. The Ac-Dex polymer was synthesized using an acetalation time of 60 min (Ac-Dex60), in order to contain in its structure a higher percentage of cyclic acetal groups than the acyclic ones.[31] Considering that the higher thermodynamic stability of the cyclic acetals generates NPs with a slow degradation rate, indeed, Ac-Dex60 is expected to release the content within 12 h. The nanoemulsion procedure was adapted[38] and optimized, in order to afford NPs with sizes of around 100 nm, in order to avoid clearance by the kidneys and liver, improve the drug pharmokinetic properties and to enhance tumor selectivity through the EPR effect.

Four different Ac-Dex NPs were prepared using a single o/w nanoemulsion procedure: (i) blank Ac-Dex NPs, (ii) Ac-Dex NPs containing the Pt^{IV} prodrug **3** (Pt^{IV}/Ac-Dex NPs), (iii) Ac-Dex NPs containing the NIR-dye **9** (NIR-dye9/Ac-Dex NPs), and (iv) Ac-Dex NPs containing both Pt^{IV} prodrug **3** and NIR-dye **9** (co-loaded Ac-Dex NPs). The size, polydispersity index (PDI) and zeta potential of the resulting nanoparticles were characterized by dynamic light scattering (DLS) (Figure 2a and Table 2). In addition, size and shape were confirmed by scanning electron microscopy (SEM, Figures 2b and 2c). For all formulations prepared, the Ac-Dex NPs obtained were spherical, with sizes ranging between 100 and 113 nm, with low dispersity (PDI < 0.155).

Due to the different solubility of the Pt^{IV} complex **3** and dye **9**, the nanoemulsion procedures to encapsulate each guest was formulated using different solvents. To encapsulate Pt^{IV} ethyl acetate was used as the organic solvent (similar to formulation of empty Ac-Dex NPs), whereas dichloromethane was used to encapsulate dye **9**. Nevertheless, minimal variability among the three distinct formulations was observed, even using different organic solvents during the preparation of blank NPs, Pt^{IV}/Ac-Dex NPs, and NIR-dye9/Ac-Dex NPs. Therefore, our data show that our formulations present a very reproducible and versatile behavior. Furthermore, the zeta potential of Ac-Dex NPs varies between -16.7 and -26.9 mV (Table 2), suggesting low tendency of the Ac-Dex NPs to aggregate in solution.

The encapsulation efficiencies (EE) of Pt^{IV} prodrug **3** and NIR dye **9** in Ac-Dex NPs were determined using ICP-OES and UV-vis spectroscopy (Table 2), respectively. When adding an initial feed of 30% (w/w) of **3** and **9** to Ac-Dex, 100% of **3** and 77% of **9** were encapsulated in the single-loaded NPs, which correspond to loading levels of 30 and 23% (w/w), respectively. Very high LC and EE were also observed by co-loaded Ac-Dex NPs. These high loadings are most likely the result from the high compatibility between the hydrophobic nature of Ac-Dex polymer and the high hydrophobicity of both guest compounds. The high drug loading capability of Ac-Dex NPs is very attractive for therapeutic applications, since high drug loading enables the use of lower amounts of nanoparticle in a given dose of treatment, as well as a lower number of doses.

Table 2. Size, polydispersity index (PDI), zeta potential, loading content (LC) and encapsulation efficiency (EE) for all Ac-Dex NPs.

Ac-Dex NPs	Size[a] (nm)	Polydispersity index	Zeta potential (mV)	Initial feed drug/polymer ratio (w/w) (%)	LC (%)	EE (%)
Blank Ac-Dex NPs	113 ± 44	0.152	-25.7 ± 3.8	--	--	--
Pt^{IV}/Ac-Dex NPs	100 ± 35	0.126	-16.7 ± 2.2	30	30 ± 0	100
NIR-dye9/Ac-Dex NPs	102 ± 38	0.137	-26.9 ± 0.4	30	23 ± 1	77
Co-loaded Ac-Dex NPs	108 ± 43	0.155	-21.1 ± 0.8	30 (Pt^{IV} complex) 2 (NIR-dye9)	30 ± 0 2 ± 0	100 100

[a]Data are presented as the mean ± standard deviation (n = 3). The standard deviation was calculated using the formula PDI = $(\sigma/D)^2$, in which PDI is the polydispersity index, σ is the standard deviation, and D is the mean diameter.

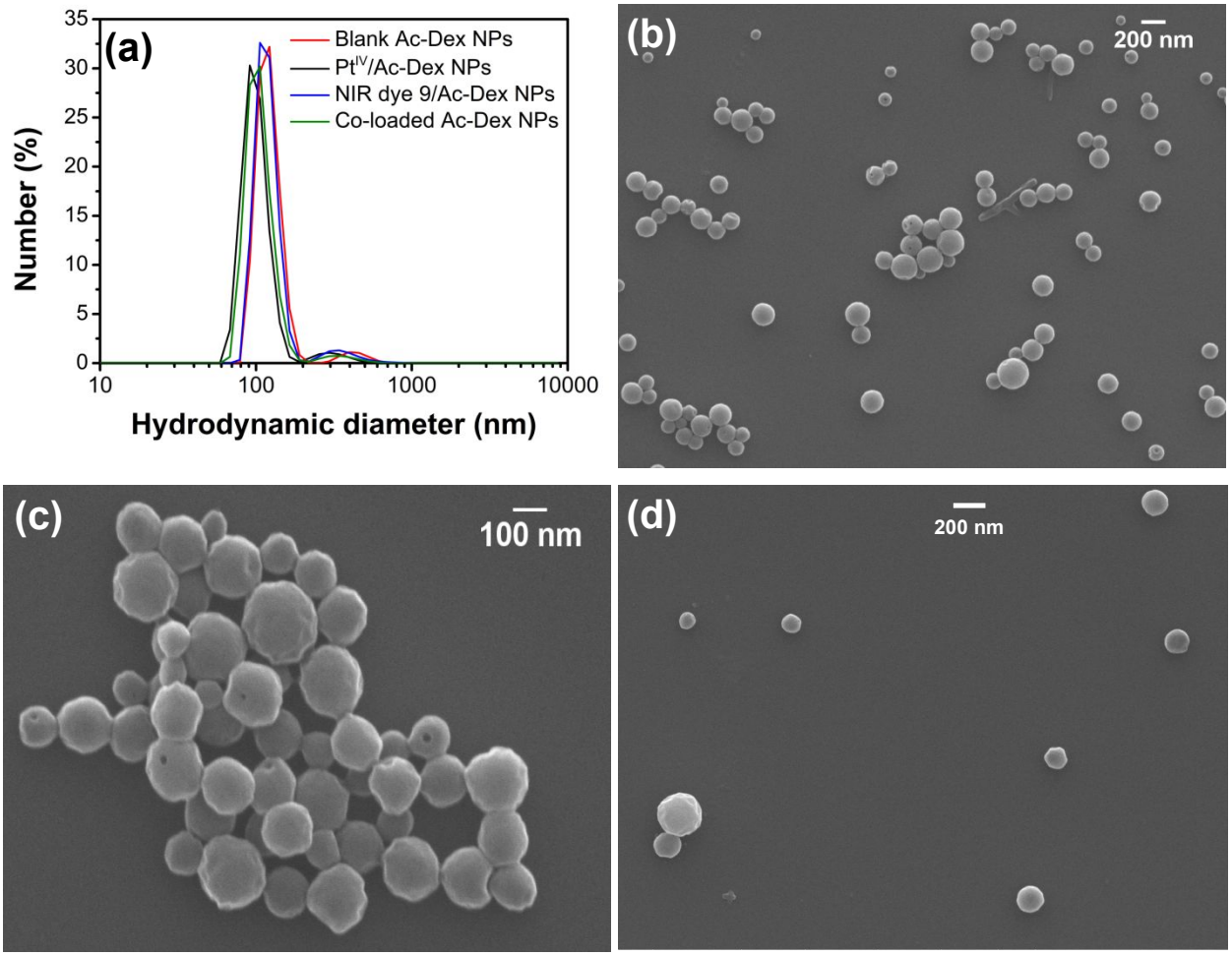

Figure 2. Size characterization of Ac-Dex NPs: (a) Size distribution of empty and loaded Ac-Dex nanoparticles by DLS. (b) SEM image of blank Ac-Dex NPs. (c) Magnified SEM image of Pt^{IV}/Ac-Dex NPs. (d) SEM image of NIR-dye9/Ac-Dex NPs.

3.4. pH-responsiveness and stability of Ac-Dex NPs

The stability of Ac-Dex NPs was evaluated in different pH conditions because pH plays an important role in storage conditions and in guest release responsiveness, which are crucial parameters in therapeutic applications. Particles were incubated *in vitro* at 37 ºC under: (i) PBS at physiological pH (pH = 7.4), (ii) cell culture medium DMEM with 10% FBS (pH = 7.4) mimicking the physiological medium, (iii) slightly alkaline water (pH = 8.0), (iv) mildly acidic aqueous solution mimicking lysosomal pH (pH = 5.5). For all medium conditions, the nanoparticles' size was monitored by DLS at predetermined time points (Figure 3). As shown in Figure 3a no significant variations in size were observed for Pt^{IV}/Ac-Dex NPs in PBS at pH 7.4 and in H_2O at pH 8.0 over three days. The particles remained in a size range of 113 - 165 nm, with changes smaller than their standard deviation, indicating that the NPs have high stability under such conditions.

When suspended in a protein-containing cell culture medium (DMEM supplemented with 10% FBS, pH 7.4) mimicking the physiological medium, the Pt^{IV}/Ac-Dex NPs increased in size within 12 h to 190 - 220 nm, which remained constant for three days. These data suggest the formation of a small protein corona in the particle surface, with low tendency to aggregate in solution, reflecting the good stability of Ac-Dex NPs in this protein-enriched medium.

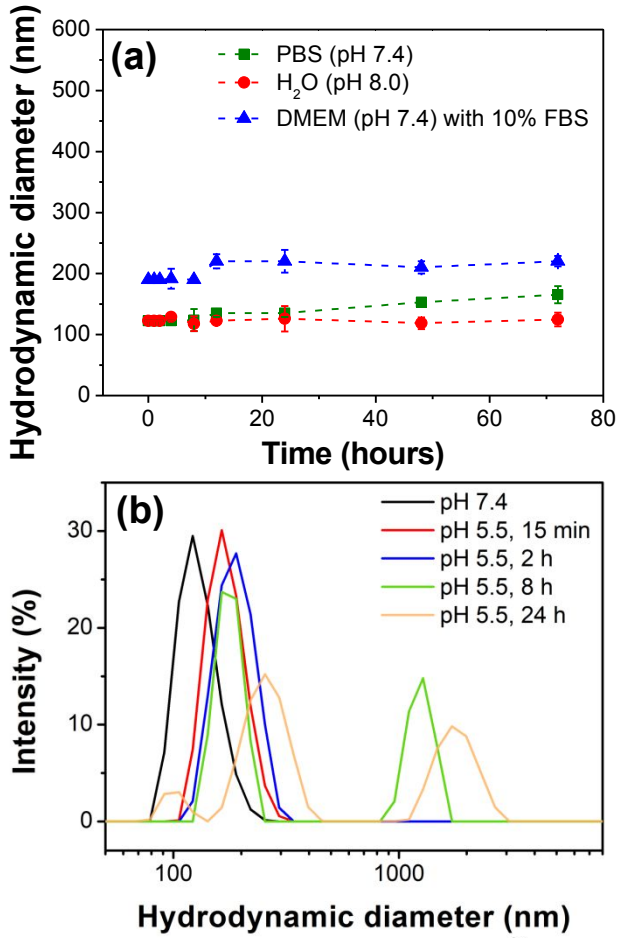

Figure 3. Stability study of Ac-Dex NPs in solution. DLS data obtained for Pt^{IV}/Ac-Dex NPs as a function of time in different media. (a) Size changes of Pt^{IV}/Ac-Dex NPs in PBS (pH 7.4), DMEM with 10% FBS (pH 7.4) and H_2O (pH 8.0) at 37 ºC in the period of 72 h measured by DLS (error bars represent the standard deviation of the mean size of three measurements). (b) Size changes of Pt^{IV}/Ac-Dex NPs at pH 7.4 and pH 5.5 at 37 ºC, over 24 h measured by DLS.

When dispersed in acetate buffer at pH 5.5 (Figure 2b), a significant increase in size of the NPs was observed within fifteen minutes up to 2 h. This change in size suggests the initial degradation of the acetal groups increasing the hydrophilicity of the polymer, and consequent disentanglement of the polymer chains and disassembly of the Ac-Dex NPs. DLS measurements after 8 and 24 h, at pH 5.5 show inconsistent results with several size populations with high dispersity, confirming the expected degradation and disassembly of the Pt^{IV}/Ac-Dex NPs in these conditions.

3.5. *In Vitro* drug release kinetics

The release profile of Pt^{IV} prodrug **3** from the pH-responsive Ac-Dex NPs was quantitatively assessed using ICP-OES at both pH 7.4 and pH 5.5, at 37 °C (Figure 4). At pH 5.5, about 80% of Pt^{IV} was released from Ac-Dex NPs within the first 12 h, whereas during this same period, only *ca*. of 15% of the prodrug **3** was released at pH 7.4. Moreover, Pt^{IV}/Ac–Dex NPs reached nearly complete release of Pt^{IV} after 72 hours at pH 5.5. In contrast, the amount of compound **3** released from the NPs after three days was lower than 25%. It is worth noting that within the first 12 hours Pt^{IV}/Ac–Dex NPs exhibit a continuous sustained release of **3** (Figure 4a, inset). A very similar release profile was observed for NIR-dye **9** from NIR-dye9/Ac-Dex NPs (Figure 4b), thus confirming that for this type of NP, the release rate is controlled by the Ac-Dex degradation in acidic environment, and it does not depend significantly on the nature of the encapsulated molecules. This release profile is suitable for anti-cancer drug delivery applications.

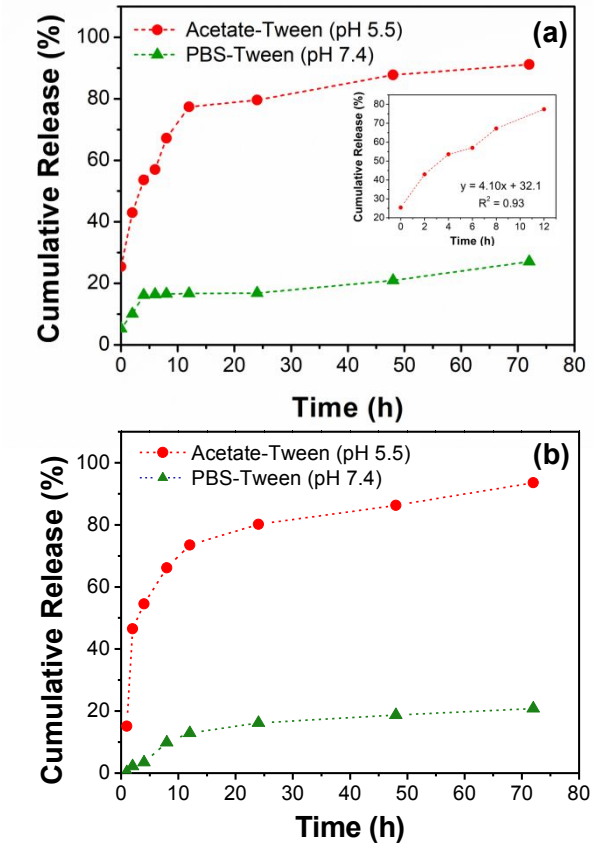

Figure 4. *In vitro* release profile of Pt^{IV} prodrug **3** from Pt^{IV}/Ac-Dex NPs (a), and dye **9** from NIR-dye **9**/Ac-Dex NPs (b), in acetate buffer-Tween (pH 5.5) and phosphate buffered saline-Tween (pH 7.4) at 37 °C.

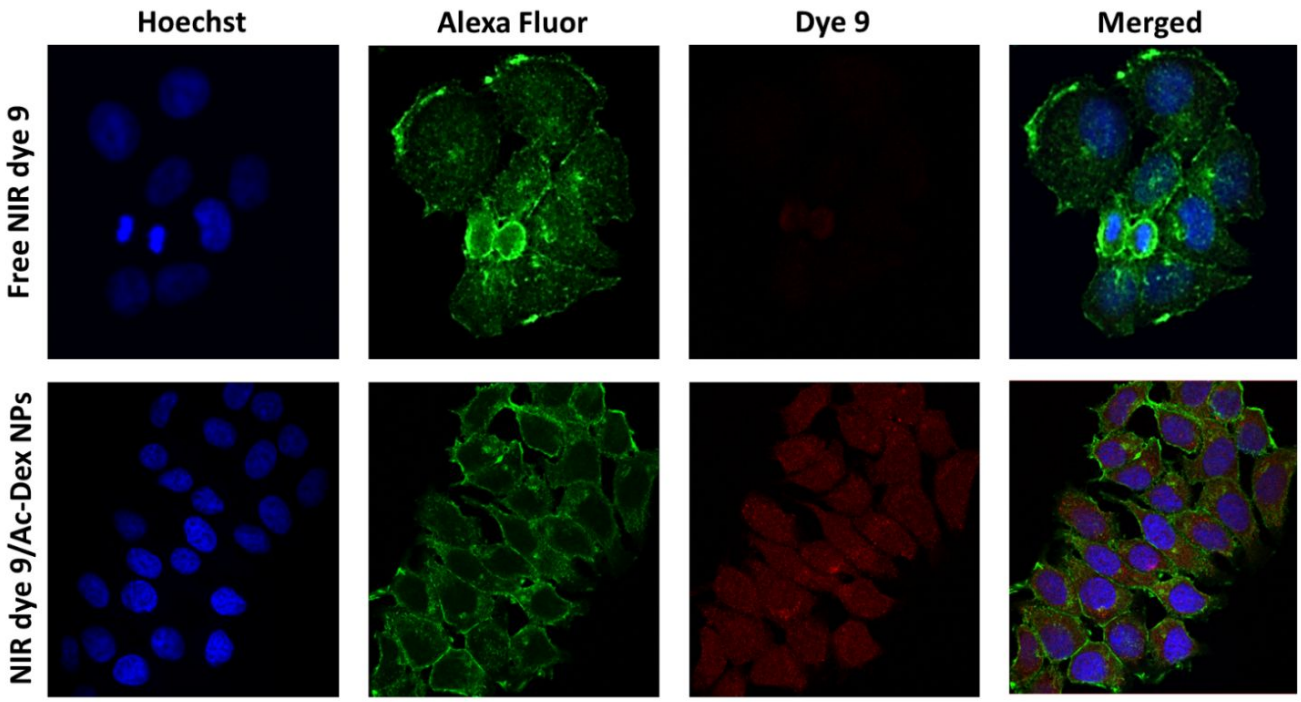

Figure 5. Comparison of cellular uptake of free and encapsulated NIR-dye **9** by observing intracellular dye **9** distribution in MCF-7 cells with confocal laser scanning microscopy. MCF-7 cells were incubated with NIR-dye **9** and with NIR-Dye9/Ac-Dex NPs for 6 h, at 37 °C. Nuclei and cytoskeleton were stained with Hoechst 33342 (blue) and Alexa Fluor 555-Phalloidin (green), respectively. The red color presented in the third channel results from dye **9** fluorescence. In both assays, the concentration of both free and encapsulated NIR-dye **9** was equivalent to 0.1 μM.

3.6. Cellular uptake by confocal microscopy

Cellular internalization of anticancer agents and nanomaterials plays a crucial role in therapeutic efficacy. To evaluate the internalization of Ac-Dex NPs, we have used the NIR-dye **9** as a fluorescent probe. The cellular uptake of the NIR-dye**9**/Ac-Dex NPs was compared with the cellular uptake of the free NIR-dye **9**. To carry out this assay, the cytotoxicity of the free and encapsulated dye was pre-determined towards different cell lines (Figures S15 and S16 of S.I.). The cytotoxicity studies clearly indicate that dye **9** and NIR-dye**9**/Ac-Dex NPs present no significant toxicity in the tested cells up to 2 μM. Therefore, the cellular uptake of dye **9** and and NIR-dye**9**/Ac-Dex NPs by MCF-7 cells was evaluated through confocal laser fluorescence microscopy (CLSM, Figure 5). The nuclei of MCF-7 cells were stained using Hoechst 33342 (presented in blue), while the cytoskeleton was stained with Alexa Fluor 555 Phalloidin (presented in green). MCF-7 cells were incubated for 6 h at 37 °C with an equal concentration (0.1 μM) of free and encapsulated dye **9** (presented in red). Upon incubation with free dye, the MCF-7 cells present a minimal intensity of NIR fluorescence, attesting a low cellular internalization of the free dye **9**. The low internalization of the free dye **9** is probably due to its highly hydrophobic nature that results in low solubility in the aqueous medium, and might enable the formation of dye aggregates that cannot penetrate efficiently the cell membrane. In contrast, MCF-7 cells incubated with NIR-dye**9**/Ac-Dex NPs, present a strong NIR fluorescence (presented in red, Figure 5). The CLSM images enabled the visualization of a homogeneous distribution pattern of the fluorescent dye in the interior of the cells delivered by the Ac-Dex NPs.

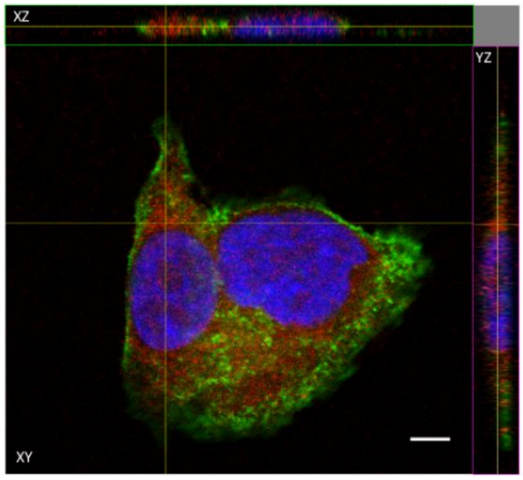

Figure 6. Orthogonal projection of confocal laser fluorescence microscopy image of MCF-7 incubated with NIR-dye**9**/Ac-Dex NPs for 6h. Blue and green colors stain the nuclei and cytoskeleton, respectively. The red fluorescence highlights the presence of NIR-dye **9** distributed within the cells.

To further confirm the cellular uptake of NIR-dye 9/Ac-Dex NPs, a z-stacking acquisition and an orthogonal projection of confocal images were performed (Figure 6). The images endorse the previous findings, indicating the successful uptake of NIR-dye **9** encapsulated in Ac-Dex NPs. Moreover, the stacked images revealed the presence of red fluorescence inside the MCF-7 nuclei, as well as in the cytoplasm. This outcome has significant importance since the mode of action of cisplatin take place in the nuclei, through the DNA-cisplatin interaction to form DNA adducts, which rises signal transduction pathways until the activation of apoptosis.[54] Altogether, these results suggest that Ac-Dex NPs are a suitable delivery platform for anticancer drugs and imaging agents.

3.7. Cytotoxic activity and IC_{50} for all compounds

The cytotoxicity of the blank and loaded Ac-Dex NPs was assessed in four different cancer cell lines: MCF-7 (breast), HeLa (cervical), Caco-2 (colon) and PC-3 (prostate), and in one healthy cell line (PNT2, prostate) using the CCK-8 assay. As showed in Figure 7, the blank Ac-Dex NPs displayed no significant cytotoxicity against all tested cell lines, even at the fairly high concentration of 1 $mg.mL^{-1}$, which exceeds the maximum concentration used during the cytotoxicity tests with loaded Pt^{IV}/Ac-Dex NPs. These results are comparable to other well-known biocompatible materials,[16] and are very promising, since the biocompatibility of delivery vehicles intended for therapeutic use is of critical importance to its eventual success.

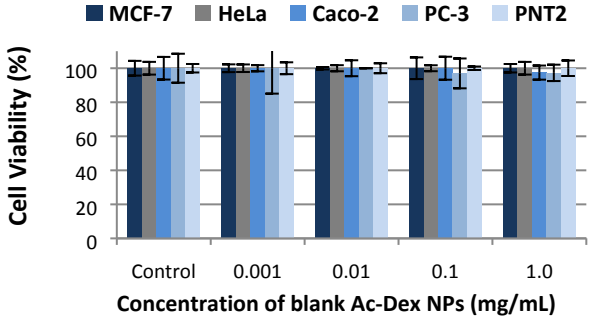

Figure 7. Cell viability data obtained for the blank Ac-Dex NPs against five different cells lines: MCF-7, HeLa, Caco-2, PC-3 and PNT2. Data were determined by CCK-8 assay and are presented as the mean from two independent experiments performed in triplicate (the bars represent the standard deviations from $n = 6$).

The cytotoxic activity of new nanosystems Pt^{IV}/Ac-Dex NPs and co-loaded Ac-Dex NPs was also assessed against MCF-7, HeLa, Caco-2, PC-3 and PNT2 cell lines, and the IC_{50} values (expressed in μM) were compared to the ones from free Pt^{IV} complex **3** and cisplatin (Table 3, Figures S17-S36 of S.I.). The free Pt^{IV} prodrug showed higher cytotoxic activity against all cell lines tested when comparing with the Pt^{II} parental compound cisplatin. Moreover, when delivered *via* the Ac-Dex polymeric nanoparticles the Pt^{IV} prodrug **3** presented much higher cytotoxic activity against all cancer cells tested when compared with the free compound. For example, free Pt^{IV} prodrug **3** and cisplatin display IC_{50} values of 2.3 and 8.3 μM for MCF-7 cells, whereas the encapsulated Pt^{IV} prodrug **3** in the Ac-Dex NPs presented an IC_{50} of around 0.2 μM in these cells. This suggest that the encapsulated prodrug **3** was about 12- and 44-fold more potent towards MCF-7 cells than the free Pt^{IV} compound and cisplatin, respectively. In PC-3 cells, the encapsulated anticancer compound (IC_{50} = 390 nM in Pt^{IV}/Ac-Dex NPs) exhibited a 6- and 41- fold higher cytotoxic activity compared to the free Pt^{IV} complex **3** (IC_{50} = 2.3 μM) and cisplatin (IC_{50} = 16.0 μM), respectively. Similar behavior in PC3 cells was showed for the Pt^{IV} complex **3** in co-loaded NPs. These results confirm the higher therapeutic efficacy of the new nanosystem when compared to both the free prodrug and cisplatin.

Table 3. IC_{50} values obtained for cisplatin, free Pt^{IV} prodrug and Pt^{IV} in Ac-Dex NPs against five cell lines.[a]

Compound	MCF-7	HeLa	Caco-2	PC3	PNT2
Cisplatin	8.3	36.9	5.9	16.0	14.7
Pt^{IV} prodrug **3**	2.3	2.9	1.1	2.3	3.5
Pt^{IV} in Pt^{IV}/Ac-Dex NPs	0.2	0.4	0.4	0.4	0.5
Pt^{IV} in co-loaded Ac-Dex NPs	0.2	0.3	0.3	0.3	0.4

[a]Cells were treated for 48 h with the indicated compounds, and the effect on cell growth was analyzed. The half-maximal inhibitory concentration (IC_{50}) is expressed in μM. Data are presented as the mean of at least one experiment carried out in triplicate. The IC_{50} values were determined from nonlinear regression analysis calculated with the GraphPad Prism 5.0 software.

CONCLUSION

We have demonstrated for the first time that Ac-Dex NPs are valid candidates as drug delivery platform for anti-cancer applications. Specifically, a Pt^{IV} prodrug (**3**), named *cis*,*cis*,*trans*-$[Pt(NH_3)_2Cl_2(CO_2(CH_2)_4CH_3)_2]$, and a tricarbocyanine derivative dye (**9**), with NIR fluorescent properties and low cytotoxicity, were efficiently encapsulated in different Ac-Dex NPs, and co-encapsulated in the Ac-Dex NPs using an oil-in-water nanoemulsion method. These NPs were obtained as small polymeric spheres with around 100 nm with low polydispersity and high encapsulation efficacy. Confocal laser fluorescence images demonstrated efficient cellular uptake Ac-Dex NPs in MCF-7 cells. Combination of the advantages of using a Pt^{IV} prodrug with the advantages of using Ac-Dex NPs resulted in a significant enhancement of the cytotoxic activity of the encapsulated Pt^{IV} prodrug against different cell lines when compared to free Pt^{IV} and cisplatin. The current results indicate that the Ac-Dex NPs provide protection for the encapsulated prodrug **3** against fast chemical or enzymatic degradation in the blood. Once the Pt^{IV}-loaded nanoparticles were internalized by cancer cells,

Pt^{IV} was released from Ac-Dex particles into the cytosol in response to the mildly acidic environment. Finally, Pt^{IV} was reduced by the intracellular medium releasing cisplatin, which inhibited DNA replication and cell proliferation. Moreover, the co-encapsulation of both the NIR-dye and the Pt^{IV} prodrug enables the possibility to use the Ac-Dex NPs for theranostics applications.

Although the cytotoxic activity of the Pt^{IV}complex is similar against prostate cancer cells (PC3) and healthy prostate cells (PNT2), it is expected that its encapsulation in 100 nm Ac-Dex NPs will result in in vivo selectivity through the EPR effect.

Overall, the easy formulation, biodegradability, biocompatibility, high drug loading capability, high encapsulation efficiency, 100 nm size, excellent stability in physiological conditions, pH-responsiveness, and tunable release rate of the Ac-Dex NPs make them a promising drug delivery platform for the selective and efficient delivery of antineoplastic drugs and imaging agents to tumor cells. Ongoing and future studies in our lab focuses on the encapsulation and co-encapsulation of different antineoplastic agents to test their anti-cancer activity *in vitro* and *in vivo*.

ASSOCIATED CONTENT

Supporting Information

The Supporting Information is available free of charge on the ACS Publications website at DOI 10.1021/acs.xxxxxxx Spectroscopic characterization of the compounds; cell viability data of the free and encapsulated NIR dye **9**; IC_{50} plots obtained for all compounds against the five cell lines (PDF).

AUTHOR INFORMATION

Corresponding Author

*E-mail: catiaornelas@catiaornelaslab.com

ORCID

Carolyne B. Braga: 0000-0003-1800-386X

Gabriel Perli: 0000-0003-2588-5100

Catia Ornelas: 0000-0001-8020-9776

Notes

The authors declare no competing financial interest.

ACKNOWLEDGMENTS

The authors gratefully acknowledge Sao Paulo Research Foundation - FAPESP (grant #2018/02093-0 for C.O.; fellowship #2017/06146-8 for C.B.B.; scholarship #2017/24488-3 for G.P.), and Coordination for the Improvement of Higher Education Personnel - CAPES (PhD scholarship for T.B.B.) for the financial support. This study was financed in part by the Coordenação de Aperfeiçoamento de Pessoal de Nivel Superior - Brasil (CAPES), finance code 001. We also thank the access to equipment and assistance provided by the National Institute of Science and Technology on Photonics Applied to Cell Biology (INFABIC) at the State University of Campinas; INFABIC is co-funded by Fundação de Amparo a Pesquisa do Estado de São Paulo (FAPESP) (08/57906-3) and Conselho Nacional de Desenvolvimento Cientifico e Tecnológico (CNPq) (573913/2008-0).

REFERENCES

1. Freitas, R. A. What is nanomedicine? *Nanomedicine: NBM* **2005,** *1*, (1), 2-9.
2. Ferrari, M.; Philibert, M. A.; Sanhai, W. R. Nanomedicine and Society. *Clin. Pharmacol. Ther.* **2009,** *85*, (5), 466-467.
3. Etheridge, M. L.; Campbell, S. A.; Erdman, A. G.; Haynes, C. L.; Wolf, S. M.; McCullough, J. The big picture on nanomedicine: the state of investigational and approved nanomedicine products. *Nanomedicine: NBM* **2013,** *9*, (1), 1-14.
4. David, A. R.; Zimmerman, M. R. Cancer: an old disease, a new disease or something in between? *Nat. Rer. Cancer* **2010,** *10*, 728-733.
5. Sun, T.; Zhang, Y. S.; Pang, B.; Hyun, D. C.; Yang, M.; Xia, Y. Engineered nanoparticles for drug delivery in cancer therapy. *Angew. Chem.* **2014,** *53*, (46), 12320-64.
6. Shi, J.; Kantoff, P. W.; Wooster, R.; Farokhzad, O. C. Cancer nanomedicine: progress, challenges and opportunities. *Nat. Rev. Cancer* **2017,** *17*, (1), 20-37.
7. Forssen, E. A.; Tökès, Z. A. Use of anionic liposomes for the reduction of chronic doxorubicin-induced cardiotoxicity. *Proc. Natl. Acad. Sci. USA* **1981,** *78*, (3), 1873-1877.
8. Ghaffar, K. A.; Giddam, A. K.; Zaman, M.; Skwarczynski, M.; Toth, I. Liposomes as Nanovaccine Delivery Systems. *Curr. Top. Med. Chem.* **2014,** *14*, (9), 1194-1208.
9. Svenson, S.; Tomalia, D. A. Commentary - Dendrimers in biomedical applications - reflections on the field. *Adv. Drug Delivery Ver.* **2005,** *57*, (15), 2106-2129.
10. Frechet, J. Dendrimers for the conjugation of small molecule drugs. *Nanomedicine: NBM* **2007,** *3*, (4), 333-333.
11. Ornelas, C.; Weck, M. Construction of well-defined multifunctional dendrimers using a trifunctional core. *Chem. Commun.* **2009**, (38), 5710-5712.
12. Astruc, D.; Boisselier, E.; Ornelas, C. Dendrimers Designed for Functions: From Physical, Photophysical, and Supramolecular Properties to Applications in Sensing, Catalysis, Molecular Electronics, Photonics, and Nanomedicine. *Chem. Ver.* **2010,** *110*, (4), 1857-1959.
13. Kannan, R. M.; Nance, E.; Kannan, S.; Tomalia, D. A. Emerging concepts in dendrimer-based nanomedicine: from design principles to clinical applications. *J. Internal Med.* **2014,** *276*, (6), 579-617.
14. Ornelas, C. Brief Timelapse on Dendrimer Chemistry: Advances, Limitations, and Expectations. *Macromol. Chem. Phys.* **2016,** *217*, (2), 149-174.
15. Li, Y.; Maciel, D.; Rodrigues, J.; Shi, X.; Tomás, H. Biodegradable Polymer Nanogels for Drug/Nucleic Acid Delivery. *Chem. Ver.* **2015,** *115*, 8564-8608.
16. Becher, T. B.; Mendonça, M. C. P.; de Farias, M. A.; Portugal, R. V.; de Jesus, M. B.; Ornelas, C. Soft Nanohydrogels Based on Laponite Nanodiscs: A Versatile Drug Delivery Platform for Theranostics and Drug Cocktails. *ACS Appl. Mater. Interfaces* **2018,** *10*, (26), 21891-21900.
17. Uhrich, K. E.; Cannizzaro, S. M.; Langer, R. S.; Shakesheff, K. M. Polymeric Systems for Controlled Drug Release. *Chem. Ver.* **1999,** *99*, (11), 3181-3198.
18. Tong, R.; Cheng, J. J. Anticancer polymeric nanomedicines. *Polym. Rev.* **2007,** *47*, (3), 345-381.
19. Daniel, M. C.; Astruc, D. Gold nanoparticles: Assembly, supramolecular chemistry, quantum-size-related properties, and applications toward biology, catalysis, and nanotechnology. *Chem. Rev.* **2004,** *104*, (1), 293-346.
20. Dykman, L. A.; Khlebtsov, N. G. Uptake of Engineered Gold Nanoparticles into Mammalian Cells. *Chem. Rev.* **2014,** *114*, (2), 1258-1288.
21. Mahapatra, A. K.; Murthy, P. N.; Samoju, S.; Mohapatra, A. K. Tiny Technology Proves Big: A Challenge at Engineering, Medicine and Pharmaceutical Sciences Interface. **2014,** *31*, (1), 1-47.
22. Patel, K.; Angelos, S.; Dichtel, W. R.; Coskun, A.; Yang, Y. W.; Zink,

J. I.; Stoddart, J. F. Enzyme-responsive snap-top covered silica nanocontainers. *J. Am. Chem. Soc.* **2008,** *130*, (8), 2382-2383.
23. Ambrogio, M. W.; Thomas, C. R.; Zhao, Y.-L.; Zink, J. I.; Stoddart, J. F. Mechanized Silica Nanoparticles: A New Frontier in Theranostic Nanomedicine. *Acc. Chem. Res.* **2011,** *44*, (10), 903-913.
24. Ornelas-Megiatto, C.; Becher, T. B.; Jr., J. D. Megiatto, Interlocked Systems in Nanomedicine *Curr. Top. Med. Chem.* **2015,** *15*, (13), 1236-1256.
25. Elsabahy, M.; Wooley, K. L. Design of polymeric nanoparticles for biomedical delivery applications. *Chem. Soc. Rev.* **2012,** *41*, (7), 2545-2561.
26. Elsabahy, M.; Heo, G. S.; Lim, S.-M.; Sun, G.; Wooley, K. L. Polymeric Nanostructures for Imaging and Therapy. *Chem. Rev.* **2015,** *115*, (19), 10967-11011.
27. Karlsson, J.; Vaughan, H. J.; Green, J. J. Biodegradable Polymeric Nanoparticles for Therapeutic Cancer Treatments. *Annu. Rev. Chem. Biomol. Eng.* **2018,** *9*, 105-127.
28. Kamaly, N.; Yameen, B.; Wu, J.; Farokhzad, O. C. Degradable Controlled-Release Polymers and Polymeric Nanoparticles: Mechanisms of Controlling Drug Release. *Chem. Rev.* **2016,** *116*, (4), 2602-63.
29. Bachelder, E. M.; Beaudette, T. T.; Broaders, K. E.; Dashe, J.; Fréchet, J. M. J. Acetal-Derivatized Dextran: An Acid-Responsive Biodegradable Material for Therapeutic Applications. *J. Am. Chem. Soc.* **2008,** *130*, (32), 10494-10495.
30. Bachelder, E. M.; Pino, E. N.; Ainslie, K. M. Acetalated Dextran: A Tunable and Acid-Labile Biopolymer with Facile Synthesis and a Range of Applications. *Chem. Rev.* **2017,** *117*, (3), 1915-1926.
31. Broaders, K. E.; Cohen, J. A.; Beaudette, T. T.; Bachelder, E. M.; Frechet, J. M. J. Acetalated dextran is a chemically and biologically tunable material for particulate immunotherapy. *Proc. Natl. Acad. Sci. USA* **2009,** *106*, (14), 5497-5502.
32. Broaders, K. E.; Cohen, J. A.; Beaudette, T. T.; Bachelder, E. M.; Fréchet, J. M. J. Acetalated dextran is a chemically and biologically tunable material for particulate immunotherapy. *Proc. Nat.l Acad. Sci. USA* **2009,** *106*, (14), 5497-5502.
33. Collier, M. A.; Junkins, R. D.; Gallovic, M. D.; Johnson, B. M.; Johnson, M. M.; Macintyre, A. N.; Sempowski, G. D.; Bachelder, E. M.; Ting, J. P.; Ainslie, K. M. Acetalated Dextran Microparticles for Codelivery of STING and TLR7/8 Agonists. *Mol. Pharmaceutics* **2018,** *15*, (11), 4933-4946.
34. Hennig, D.; Schubert, S.; Dargatz, H.; Kostenis, E.; Fahr, A.; Schubert, U. S.; Heinzel, T.; Imhof, D. Novel insights into appropriate encapsulation methods for bioactive compounds into polymers: a study with peptides and HDAC inhibitors. *Macromol. Biosci.* **2014,** *14*, (1), 69-80.
35. Peine, K. J.; Guerau-de-Arellano, M.; Lee, P.; Kanthamneni, N.; Severin, M.; Probst, G. D.; Peng, H.; Yang, Y.; Vangundy, Z.; Papenfuss, T. L.; Lovett-Racke, A. E.; Bachelder, E. M.; Ainslie, K. M. Treatment of experimental autoimmune encephalomyelitis by codelivery of disease associated Peptide and dexamethasone in acetalated dextran microparticles. *Mol. Pharmaceutics* **2014,** *11*, (3), 828-35.
36. Bachelder, E. M.; Beaudette, T. T.; Broaders, K. E.; Frechet, J. M.; Albrecht, M. T.; Mateczun, A. J.; Ainslie, K. M.; Pesce, J. T.; Keane-Myers, A. M. In vitro analysis of acetalated dextran microparticles as a potent delivery platform for vaccine adjuvants. *Mol. Pharmaceutics* **2010,** *7*, (3), 826-35.
37. Kauffman, K. J.; Kanthamneni, N.; Meenach, S. A.; Pierson, B. C.; Bachelder, E. M.; Ainslie, K. M. Optimization of rapamycin-loaded acetalated dextran microparticles for immunosuppression. *Int. J. Pharmaceutics* **2012,** *422*, (1-2), 356-63.
38. Ornelas-Megiatto, C.; Shah, P. N.; Wich, P. R.; Cohen, J. L.; Tagaev, J. A.; Smolen, J. A.; Wright, B. D.; Panzner, M. J.; Youngs, W. J.; Fréchet, J. M. J.; Cannon, C. L. Aerosolized Antimicrobial Agents Based on Degradable Dextran Nanoparticles Loaded with Silver Carbene Complexes. *Mol. Pharmaceutics* **2012,** *9*, (11), 3012-3022.
39. Cohen, J. A.; Beaudette, T. T.; Cohen, J. L.; Broaders, K. E.; Bachelder, E. M.; Fréchet, J. M. J. Acetal-Modified Dextran Microparticles with Controlled Degradation Kinetics and Surface Functionality for Gene Delivery in Phagocytic and Non-Phagocytic Cells. *Adv. Mater.* **2010,** *22*, (32), 3593-3597.
40. Cohen, J. L.; Schubert, S.; Wich, P. R.; Cui, L.; Cohen, J. A.; Mynar, J. L.; Fréchet, J. M. J. Acid-Degradable Cationic Dextran Particles for the Delivery of siRNA Therapeutics. *Bioconjugate Chem.* **2011,** *22*, (6), 1056-1065.
41. Johnson, M. M.; Collier, M. A.; Hoang, K. V.; Pino, E. N.; Graham-Gurysh, E. G.; Gallovic, M. D.; Zahid, M. S. H.; Chen, N.; Schlesinger, L.; Gunn, J. S.; Bachelder, E. M.; Ainslie, K. M. In Vivo and Cellular Trafficking of Acetalated Dextran Microparticles for Delivery of a Host-Directed Therapy for Salmonella enterica Serovar Typhi Infection. *Mol. Pharmaceutics* **2018,** *15*, (11), 5336-5348.
42. Wong, E.; Giandomenico, C. M. Current Status of Platinum-Based Antitumor Drugs. *Chem. Rev.* **1999,** *99*, (9), 2451-2466.
43. Kim, J.; Pramanick, S.; Lee, D.; Park, H.; Kim, W. J. Polymeric biomaterials for the delivery of platinum-based anticancer drugs. *Biomater. Sci.* **2015,** *3*, (7), 1002-17.
44. Johnstone, T. C.; Suntharalingam, K.; Lippard, S. J. The Next Generation of Platinum Drugs: Targeted Pt(II) Agents, Nanoparticle Delivery, and Pt(IV) Prodrugs. *Chem. Rev.* **2016,** *116*, (5), 3436-86.
45. Kelkar, S. S.; Reineke, T. M. Theranostics: Combining Imaging and Therapy. *Bioconjugate Chem.* **2011,** *22*, (10), 1879-1903.
46. Svenson, S. Theranostics: Are We There Yet? *Mol. Pharmaceutics* **2013,** *10*, (3), 848-856.
47. Hall, M. D.; Dillon, C. T.; Zhang, M.; Beale, P.; Cai, Z.; Lai, B.; Stampfl, A. P.; Hambley, T. W. The cellular distribution and oxidation state of platinum(II) and platinum(IV) antitumour complexes in cancer cells. *J. Biol. Inorg. Chem.* **2003,** *8*, (7), 726-32.
48. Nascimento, A. V.; Singh, A.; Bousbaa, H.; Ferreira, D.; Sarmento, B.; Amiji, M. M. Combinatorial-Designed Epidermal Growth Factor Receptor-Targeted Chitosan Nanoparticles for Encapsulation and Delivery of Lipid-Modified Platinum Derivatives in Wild-Type and Resistant Non-Small-Cell Lung Cancer Cells. *Mol. Pharmaceutics* **2015**, *12*, (12), 4466-77.
49. Dhar, S.; Gu, F. X.; Langer, R.; Farokhzad, O. C.; Lippard, S. J. Targeted delivery of cisplatin to prostate cancer cells by aptamer functionalized Pt(IV) prodrug-PLGA-PEG nanoparticles. *Proc. Natl. Acad. Sci. USA* **2008,** *105*, (45), 17356-61.
50. Bisht, R.; M, K. M.; Singh, A. K.; Nithyanandhan, J. Panchromatic Sensitizer for Dye-Sensitized Solar Cells: Unsymmetrical Squaraine Dyes Incorporating Benzodithiophene pi-Spacer with Alkyl Chains to Extend Conjugation, Control the Dye Assembly on TiO2, and Retard Charge Recombination. *J. Org. Chem.* **2017,** *82*, (4), 1920-1930.
51. Mishra, A.; Behera, R. K.; Behera, P. K.; Mishra, B. K.; Behera, G. B. Cyanines during the 1990s: A Review. *Chem. Rev.* **2000,** *100*, (6), 1973-2012.
52. Ornelas, C.; Lodescar, R.; Durandin, A.; Canary, J. W.; Pennell, R.; Liebes, L. F.; Weck, M. Combining aminocyanine dyes with polyamide dendrons: a promising strategy for imaging in the near-infrared region. *Chem. Eur. J.* **2011,** *17*, (13), 3619-29.
53. Peng, X.; Song, F.; Lu, E.; Wang, Y.; Zhou, W.; Fan, J.; Gao, Y. Heptamethine cyanine dyes with a large stokes shift and strong fluorescence: a paradigm for excited-state intramolecular charge transfer. *J. Am. Chem. Soc.* **2005,** *127*, (12), 4170-1.
54. Siddik, Z. H. Cisplatin: mode of cytotoxic action and molecular basis of resistance. *Oncogene* **2003,** *22*, (47), 7265-79